Electromechanical modelling and *in silico* analysis of a rat cardiac syncytium

Fabrizio Del Bianco[1,2], Piero Colli Franzone[3], Simone Scacchi[4], and Lorenzo Fassina[1,2]
[1] *Department of Industrial and Information Engineering, University of Pavia, Pavia, Italy*
[2] *Centre for Tissue Engineering (C.I.T.), University of Pavia, Pavia, Italy*
[3] *Department of Mathematics, University of Pavia, Pavia, Italy*
[4] *Department of Mathematics, University of Milano, Milano, Italy*

***Abstract*—In this paper we studied the mechanics and physiology occurring during the contraction of a 2D syncytium made of rat cardiomyocytes by carrying out numerical simulations of an electromechanical model for its cell and tissue components. Our model was qualitatively compared with experimental results taken from literature and it gave us optimistic outputs providing a tool for future studies into cardiac mechanisms and contraction even in a 3D environment.**

***Keywords*—Cardiac modelling, Rat syncytium, Mechanics, Physiology.**

I. Introduction

A large amount of experimental data is almost available for researchers focused on studying heart movements at different time and spatial scales from genomic description up to whole-organ context. Mathematical modelling may help them to unify biological data. New and more detailed models can be built from simpler ones, which can be available on an online database like *CellML 1.1*. In particular, we took three different models describing rat cardiac phenomena at the cell scale, which had already been corrected and integrated into the so-called PHN (Pandit-Hinch-Niederer) model: Pandit *et al.* electrical activity model [1], Hinch *et al.* calcium dynamics model [2] and Niederer *et al.* active tension (or contraction force) generation model [3]. Actually a full cardiac cell electromechanical model is composed of at least two components: a bioelectrical model describing the development of the action potential and a model for the excitation-contraction coupling focusing on the way the electrical stimulus is converted into the contraction of the cardiomyocyte, i.e. a model describing how calcium moves across different intracellular compartments and a model describing the mechanisms underlying the generation of the contraction force. Then, in order to simulate the electromechanical response of our 2D layer of cardiac tissue, we added a monodomain model [4] to allow the propagation of the action potential and a quasi-static finite elastic model [5][6] to simulate biomechanical aspects at the tissue scale. At last we planned a set of simulations changing the values of some relevant parameters in order to better match the experimental results we found from literature [7][8][9].

II. Methods

A. The electrophysiological model

Electrophysiology was modelled by the monodomain representation of cardiac tissue [4] coupled with the PHN model giving:

$$\begin{cases} c_m \dfrac{\partial V}{\partial t} - \dfrac{1}{J}\mathrm{Div}(J\mathbf{F}^{-1}\mathbf{D}\mathbf{F}^{-T}\mathrm{Grad}\, V) + i_{ion}(V,w,c) = i_{app} & \text{in } \Omega_0 \times (0,T) \\ \dfrac{\partial w}{\partial t} - M(V,w) = 0 & \text{in } \Omega_0 \times (0,T) \\ \dfrac{\partial c}{\partial t} - S(V,w,c) = 0 & \text{in } \Omega_0 \times (0,T) \\ \mathbf{n}^T\mathbf{F}^{-1}\mathbf{D}\mathbf{F}^{-T}\mathrm{Grad}\, V = 0 & \text{in } \partial\Omega_0 \times (0,T) \\ V(\mathbf{x},0) = V_0(\mathbf{x}), \quad w(\mathbf{x},0) = w_0(\mathbf{x}), \quad c(\mathbf{x},0) = c_0(\mathbf{x}) & \text{in } \Omega_0, \end{cases} \tag{1}$$

where V is the transmembrane potential, w and c are vectors containing gating variables or ionic intracellular concentrations respectively belonging to the PHN model together with their initial conditions on the last line, c_m is the membrane capacitance, J is the determinant of the deformation gradient tensor $\boldsymbol{F}$ for mechanics, $\boldsymbol{D}$ is the bulk conductivity tensor and it accounts for myocardium electrical anisotropy, i_{ion} is the total ionic current and i_{app} is the applied current stimulus. The fourth equation is a zero Neumann boundary condition because we assumed that our myocardium layer was electrically isolated. This evolution system referred to tissue initial (not deformed) configuration Ω_0 as it is usually required by solid deformation analysis.

B. The mechanical model

In a quasi-static regime without body external forces the equilibrium condition is given by [5]:

$$\mathrm{Div}\ \mathbf{FS} = \mathbf{0}, \tag{2}$$

where $\boldsymbol{S}$ is the symmetric second Piola-Kirchhoff stress tensor. $\boldsymbol{S}$ contained both an active component $\boldsymbol{S}^{act}$ related to cell active tension T_a and a passive component $\boldsymbol{S}^{pas}$, whose equation depended on a suitable myocardium strain energy function W and on a quasi-incompressibility term $\boldsymbol{S}^{vol}$ [6]. Assuming a 2D layer of tissue made up with parallel fibers, the full expression of $\boldsymbol{S}$ was:

$$S_{MN} = \frac{T_a}{C_{11}}\delta_{M1}\delta_{N1} + \frac{1}{2}\left(\frac{\partial W}{\partial E_{MN}} + \frac{\partial W}{\partial E_{NM}}\right) - S^{vol}_{MN}, \tag{3}$$

where $\boldsymbol{C}$ is the Cauchy-Green deformation tensor, $\delta_{M1}\delta_{N1}$ ensures that the force acted only along the x-axis of fiber direction and $\boldsymbol{E}$ is the Lagrange-Green strain tensor. For the function W we adopted the Guccione exponential law [5], which treats the cardiac material as mechanically anisotropic:

$$W = \frac{1}{2}a\left(e^{b_1E_{11}^2 + b_2E_{22}^2 + 2b_3E_{12}^2} - 1\right), \tag{4}$$

where a, b_1, b_2 and b_3 are fixed parameters.

C. Geometry of tissue and model implementation

Simulations were carried out in Matlab on a 1 cm × 1 cm square layer of tissue. The left edge was fixed during all time

of simulations (T = 10000 ms). External stimuli were delivered near the central part of the lowest edge to generate action potentials that spread throughout the layer. For electrical components we used a uniform fine mesh of 64 × 64 Q_1 finite elements (giving us a nodal spacing of 0.015625 cm) and a time step of 0.05 ms. For mechanical components we limited to a uniform coarser mesh of 8 × 8 Q_1 finite elements (giving us a nodal spacing of 0.125 cm) and to a time step of 1 ms because tissue contraction is often much slower than electrical propagation. The discretization of the complete model was performed by finite elements in space and semi-implicit finite differences in time [4].

III. Results and Discussion

We chose nine equidistant nodes belonging to a 3 × 3 square grid central to the fine mesh as markers for simulation results. We saved their *(x,y)* coordinates and their corresponding values for active tension T_a, intracellular calcium concentration $[Ca]_i$ and deformation λ every 0.05 ms. Fig. 1 shows some frames and the superimposed markers grid of a sample simulation movie for our square layer. All previous values were processed in Matlab again to give us the following results for mechanics and physiology.

A. Trajectories

Fig. 2 displays the trajectory described by a sample marker during a simulation. A typical contraction/relaxation cycle was characterized by four phases [7]. In phase 1 the marker velocity was minimum but the acceleration became higher and higher and the marker started to move. During phase 2 the marker reached its maximum contraction velocity and its minimum acceleration. At the end of its contraction in phase 3, the marker velocity became minimum again whereas its deceleration got the maximum value and the marker reached its farthest position from its starting point. At last, during phase 4, the marker first gained its maximum relaxation velocity and then came back to its original position where its velocity was minimum. During its movement the marker described a typical hysteresis cycle because paths in phases 2 and 4 were not the same.

B. Force-Frequency Relationship

In Fig. 3 and Fig. 4 we analysed the FFR (Force-Frequency Relationship), also called rate staircase, which represents an important intrinsic mechanism for cardiac contractility [8]. Fig. 3 shows this phenomenon as an average among all marker values for maximum steady-state active tension T_a with an extracellular calcium concentration $[Ca]_o$ = 1 mM. We found a first positive phase between 0.625 Hz and 0.83 Hz, where the higher the frequency f was the more active tension raised, a second flat phase between 0.83 Hz and 1.6 Hz, where a frequency increase did not alter active tension and a third negative phase between 1.6 Hz and 2.5 Hz, where frequency raised but active tension decreased. Instead by increasing $[Ca]_o$ to 4 mM we observed approximately an opposite response as shown in Fig. 4.

C. Frank-Starling law

In Fig. 5 we studied another important intrinsic cardiac mechanism, i.e. the Frank-Starling law, according to which the more cardiomyocytes are initially stretched the more they develop contractile force T_a within a physiological range [9]. Our model gave us these results because the peak active tension in time during the last beat increased if values for deformation λ were higher but were still physiological (maximum λ was set to 1.1 corresponding to sarcomere length of about 2.1 μm).

IV. Conclusion

Our model for a 2D rat cardiac tissue layer gave us results in agreement with most of experimental features though our modelling exhibits various limitations, which might be overtaken in future studies. Pandit *et al.* model is affected by saturation phenomena when frequencies are higher than 3 ÷ 4 Hz, so we were not allowed to study the cardiac behaviour near rat physiological frequencies (between 5 Hz and 9 Hz). Moreover all PHN parameters were calibrated at room temperature (22°C), so we could not compare our results with the experimental ones at physiological temperature (37°C). However our 2D model may be a first step to better explain cultured cardiomyocytes movement on Petri dishes. It could be turned into a 3D one, which would take into account culture thickness too, since layers contract in different ways according to their depth. Moreover the same framework could be applied to the study of human cardiac tissue by replacing the rat cell model with a human one (if possible, already available on *CellML 1.1*) and changing the values of the parameters belonging to the electrophysiological and mechanical models. This initial estimation procedure and the final validation of our model results may benefit from electrical and mechanical *in vitro* experiments on cardiac fibers that beat under conditions similar to those simulated.

References

[1] S. V. Pandit, R. B. Clark, W. R. Giles, and S. S. Demir, "A mathematical model of action potential heterogeneity in adult rat left ventricular myocytes," *Biophysical Journal*, vol. 81, pp. 3029–3051, December 2001.

[2] R. Hinch, J. L. Greenstein, A. J. Tanskanen, L. Xu, and R. L. Winslow, "A simplified local control model of calcium-induced calcium release in cardiac ventricular myocytes," *Biophysical Journal*, vol. 87, pp. 3723–3736, December 2004.

[3] S. A. Niederer, P. J. Hunter, and N. P. Smith, "A quantitative analysis of cardiac myocyte relaxation: a simulation study," *Biophysical Journal*, vol. 90, pp. 1697–1722, March 2006.

[4] P. Colli Franzone and L. F. Pavarino, "A parallel solver for reaction-diffusion systems in computational electrocardiology," *Mathematical Models and Methods in Applied Sciences*, 14, pp. 883–911, 2004.

[5] G. A. Holzapfel and R. W. Ogden, "Constitutive modelling of passive myocardium: a structurally based framework for material characterization," *Phil. Trans. R. Soc.*, vol. 367, pp. 3445–3475, August 2004.

[6] P. Pathmanathan and J. P. Whiteley, "A numerical method for cardiac mechanoelectric simulations," *Annals of Biomedical Engineering*, vol. 37, pp. 860–873, May 2009

[7] L. Fassina et al., "Video evaluation of the kinematics and dynamics of the beating cardiac syncytium: an alternative to the Langendorff method," *Int. J. Artif. Organs*, vol. 34, pp. 546–558, March 2011.

[8] J. Layland and J. C. Kentish, "Positive force- and $[Ca^{2+}]_i$-frequency relationships in rat ventricular trabeculae at physiological frequencies," *Am. J. Physiol. Heart Circ. Physiol.*, vol. 276, pp. H9–H18, 1999.

[9] P. M. L. Janssen, L. B. Stull, and E. Marban, "Myofilament properties comprise the rate-limiting step for cardiac relaxation at body temperature in the rat," *Am. J. Physiol. Heart Circ. Physiol.*, vol. 282, pp. H499–H507, 2002.

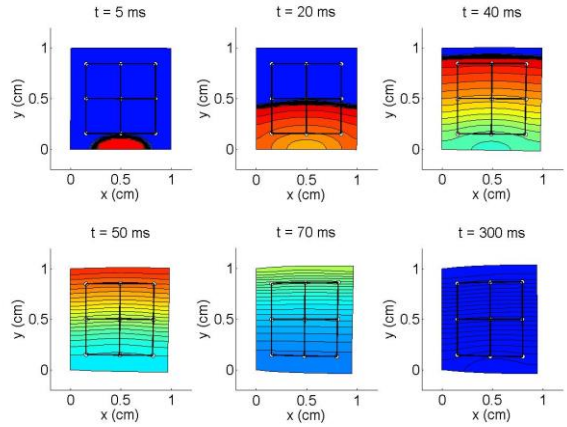

Fig. 1. Movie frames of a sample simulation with beat frequency f = 2.5 Hz and extracellular calcium concentration $[Ca]_o$ = 1 mM. Different colours stand for more or less depolarized fine mesh nodes (more positive transmembrane potential V values tending to red and more negative ones tending to blue), black lines that split colours are the equipotential lines and white dots are the nine markers of the superimposed grid.

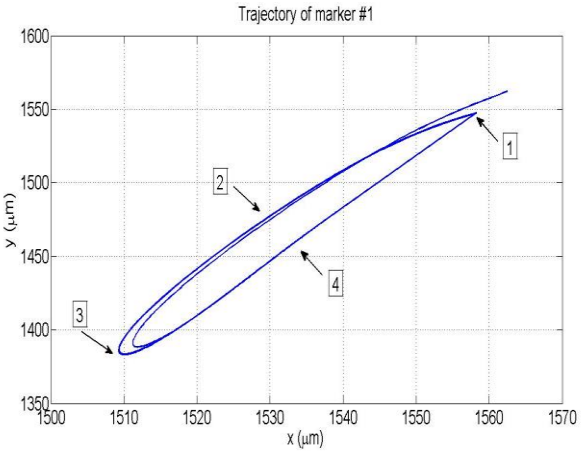

Fig. 2. Trajectory in the plane x-y described by an example marker with beat frequency f = 0.625 Hz and extracellular calcium concentration $[Ca]_o$ = 1 mM. Numbers point out the four phases of a contraction/relaxation cycle.

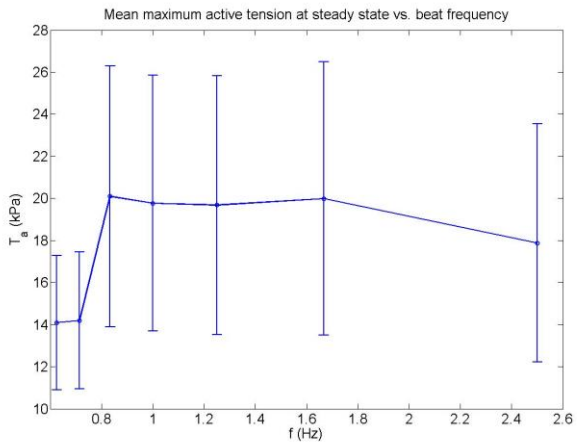

Fig. 3. Maximum steady-state active tension T_a values averaged over all markers for different values of beat frequency f with extracellular calcium concentration $[Ca]_o$ = 1 mM. Circles stand for mean values and vertical bars for standard deviations.

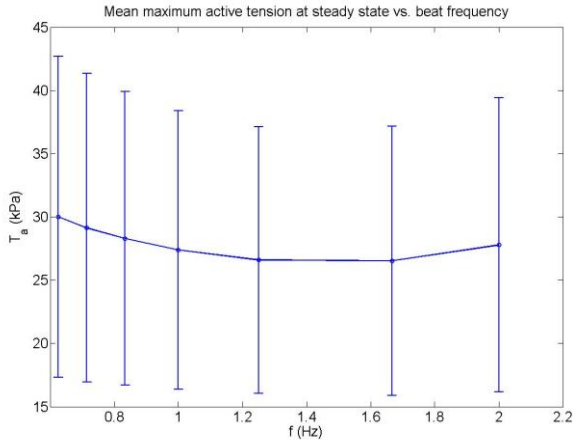

Fig. 4. Maximum steady-state active tension T_a values averaged over all markers for different values of beat frequency f with extracellular calcium concentration $[Ca]_o$ = 4 mM. Circles stand for mean values and vertical bars for standard deviations.

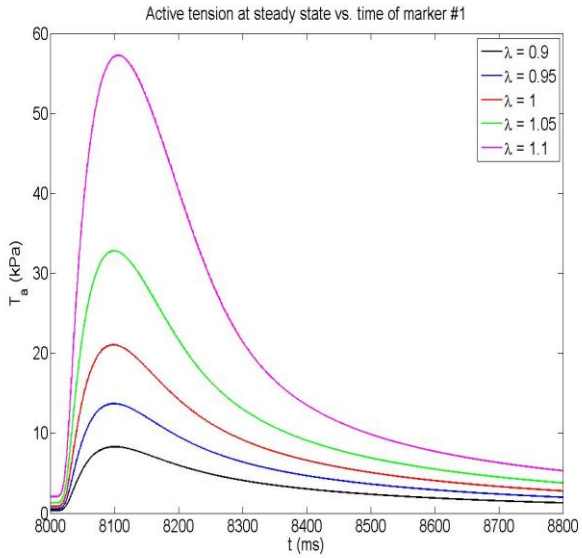

Fig. 5. Time evolution of active tension T_a for different values of deformation λ at steady state for an example marker with beat frequency f = 0.5 Hz and extracellular calcium concentration $[Ca]_o$ = 1 mM.